

CP-violating HWW couplings at the Large Hadron Collider

Nishita Desai and Biswarup Mukhopadhyaya

Harish-Chandra Research Institute, Jhansi, Allahabad - 211 019, India

Dilip Kumar Ghosh

Department of Theoretical Physics,

Indian Association for Cultivation of Science,

2A & 2B Raja S.C. Mullick Road,

Kolkata - 700032 , India

Abstract

We investigate the possibility of probing an anomalous CP-violating coupling in the HWW vertex at the LHC. We consider the production of the Higgs in association of a W and then decay via the $H \rightarrow WW$ channel taking into account the limits on the Higgs production cross section from the Tevatron. We select the same-sign dilepton final state arising from leptonic decays of two of the three Ws and apply cuts required to suppress the standard model background. Several kinematical distributions and asymmetries that can be used to ascertain the presence of a non-zero anomalous coupling are presented. We find that, for Higgs mass in the range 130-150 GeV and anomalous couplings allowed by the Tevatron data, these distributions can be studied with an integrated luminosity of 30-50 fb⁻¹ at the 14 TeV run. Attention is specifically drawn to some asymmetries that enable one to probe the real and imaginary parts (as well as their signs) of the anomalous coupling, in a complementary manner. We also explicitly demonstrate that showering and hadronisation do not affect the utility of these variables, thus affirming the validity of parton level calculations.

I. INTRODUCTION

The most well-motivated explanation for electroweak symmetry breaking is via the Higgs mechanism. Although the Higgs boson remains the only unobserved particle in the Standard Model (SM), there are both experimental and theoretical bounds on its mass. The LEP bound of 114 GeV has now been supplemented with the Tevatron bounds which rule out Higgs masses between 158 – 173 GeV [1, 2].

Here we consider the possibility of the Higgs boson existing somewhere between 130 – 150 GeV where the decay width of $H \rightarrow WW$ is appreciable. This is the range which has not yet been ruled out by the Tevatron and is likely to be probed at the earliest at the Large Hadron Collider (LHC)[3, 4]. On the one hand, there is substantial rate of production; on the other, the viability of the WW^* decay channel avoids the requirement of the two-photon mode, and consequently the requirement of a large integrated luminosity for discovery.

In such a situation, we wish to probe whether the HWW -coupling is purely described by the standard model. Such couplings can be probed in the relatively clean leptonic channels and previous studies for HWW and HZZ couplings at the LHC can be found in [5–11]. Many studies for both HWW and HZZ anomalous couplings also exist in the context of a future e^+e^- collider [12–17], $e\gamma$ collider [18] and photon collider [19, 20]. LEP limits on anomalous Higgs couplings can be found in [21].

The primary production channel at the LHC is through gluon-gluon fusion and would in principle be the cleanest to probe the HWW vertex. However, the decay $H \rightarrow W^+W^-$ leads to an opposite-sign dilepton signature which is prone to large backgrounds from $pp \rightarrow W^+W^-$. This background is generally eliminated by removing back-to-back leptons with an appropriate cut[22]. However, these cuts are no longer useful when one wishes to probe the presence of anomalous couplings because the difference made by the anomalous couplings in angular distributions of dilepton events is often in this kinematic region. We therefore choose to probe the associated production channel instead. A study for probing the anomalous couplings in the vector-boson fusion channel can be found in [23]. One could also consider Higgs production via $pp \rightarrow ZH$. However, if the HWW vertex has anomalous couplings, it would be natural to expect the HZZ vertex to also have such couplings. In that case, one is left to disentangle the interference of both HWW and HZZ vertices and this will further complicate the study of the HWW interaction.

Thus we explore the production of the Higgs via $pp \rightarrow WH$, and its subsequent decay, again through the HWW coupling. The interplay of anomalous coupling in both the production and decay vertices makes the resulting phenomenology richer and more complicated, but free from contamination from other effects. The environment of a hadron collider and the presence of two neutrinos in the final decay products makes the reconstruction of the event and the extraction of a non-standard HWW vertex difficult. However, as we shall see, there are significant differences in angular distributions which may point to the presence of anomalous contributions. We will also specifically address the issue of effect of initial and final state radiation on the variables as this is a fundamental concern at the LHC.

The paper is organised as follows. In the next section, we acquaint the reader with the anomalous couplings, and go on to discuss model-independent strategies for probing the CP-violating anomalous coupling, in a parton level Monte Carlo approach. Our event selection criteria are also discussed there. Section III contains our numerical results, including various distributions and asymmetries relevant for the analysis. In section IV, we report the results of a study where hadronisation and initial and final state radiation are included, and try to convince the reader that these do not alter the conclusions of a parton level study in most cases. Our conclusions are presented in section V.

II. THE ANOMALOUS COUPLING AND ITS SIMULATION

The HWW vertex can receive corrections from higher dimensional operators like $\frac{(\Phi^\dagger \Phi)}{\Lambda^2} W_{\mu\nu} W^{\mu\nu}$ and $\frac{(\Phi^\dagger \Phi)}{\Lambda^2} W_{\mu\nu} \tilde{W}^{\mu\nu}$. The general HWW vertex may then be written in a model-independent way as $\Gamma_{\mu\nu} W^\mu W^\nu H$ where:

$$\Gamma_{\mu\nu} = \frac{igM_W}{2} \left(ag_{\mu\nu} + \frac{b}{M_W^2} (p_{1\mu} p_{2\nu} + p_{1\nu} p_{2\mu} - (p_1 \cdot p_2) g_{\mu\nu}) + \frac{\tilde{b}}{M_W^2} \epsilon_{\mu\nu\rho\sigma} p_1^\rho p_2^\sigma \right) \quad (1)$$

where p_1 and p_2 are the momenta of the two gauge bosons. For this study, we assume a completely phenomenological origin of b and \tilde{b} . The Standard Model vertex then corresponds to $b = 0$, $\tilde{b} = 0$ and $a = 1$. We particularly wish to investigate the effect of non-zero values of \tilde{b} which would lead to CP -violation. Therefore, we set b to zero all along. We also include the possibility of a complex \tilde{b} , arising out of some absorptive part in the effective interaction.

A. Simulation

To start, a parton-level Monte Carlo analysis has been performed for investigating the kinematical consequences of the CP-violating anomalous vertex at the LHC, using leptons in the final state. In section IV, we will show that the results of this simplified analysis are not altered by showering and hadronisation effects. We factorize the entire matrix element into two pieces $pp \rightarrow H\ell\nu(\ell = e, \mu)$ and $H \rightarrow WW^* \rightarrow \ell\nu\bar{f}f'$ [24]. Since the Higgs is a scalar, we expect that this does not affect the spin correlations. Both matrix elements have been calculated using Form [25]. For the first part of our study, we perform a simple smearing of the lepton momenta to approximate detector effects with a Gaussian of width given by $\sigma(E) = aE + b\sqrt{E}$ with $a = 0.02$ and $b = 0.05$ [33]. The lepton identification efficiency has been assumed to be 100%.

We present our calculations for a proton-proton centre-of-mass energy of 14 TeV. The signal rates are too small at 7 TeV to be accessible at the current run with the projected luminosity. The cross section is calculated using the CTEQ6L1 parton distribution functions[26] using with the renormalisation and factorisation scales both set at $\sqrt{\hat{s}}$, the subprocess centre-of-mass energy.

The modification of the leading order (LO) decay width in the $H \rightarrow f\bar{f}'\bar{f}f'$ channel has also been calculated and taken into account in each case. We focus on same-sign dileptons (SSD), when only one of the W s from the Higgs decays leptonically. It is less profitable to look into exclusive opposite-sign dilepton because of the large background from W^+W^- production. In Higgs searches, this background is generally suppressed using a cut on the angle between the two leptons — the ones from W^+W^- production are mostly back-to-back whereas those from Higgs decay are highly collimated. Since the excess events due to the term proportional to \tilde{b} tend to also increase the angle between the opposite-sign leptons, we cannot really use this as a criterion for cutting out the background. We can also look at trilepton states when both the W s decay into leptonic final states but we omit them for this work due to very low cross sections.

The Tevatron has certain bounds on the cross section of Higgs production. The latest CDF bounds in the SSD channel with 7.1 fb^{-1} data on the ratio of the Higgs production cross section to the SM rate in the electron and muon channels are 9.63 (4.99) on Higgs masses of 130 (150) GeV[27]. The combined CDF and DØ results[1] put a much stronger upper

bound on the Higgs cross sections by combining various channels. However, the anomalous coupling affects only the production via the associated WH production for which the bounds are not as strong. We present the results in our paper for a value $|\tilde{b}| = 0.2$ which satisfies the above CDF bounds.

B. Backgrounds and Cuts

At the LHC, the largest contribution to the background for SSD comes from semileptonic B -meson decays in $b\bar{b}$ production where one of the B -mesons oscillates into its charge conjugate state. It has been well-known for some time that the isolation cuts alone are not enough to suppress this background[28] but an additional cut on the transverse momentum (p_T) is required. We found that demanding an additional p_T -cuts along with a cut on missing transverse energy (E_T) is very effective for suppressing this background. We require two isolation cuts on the leptons, viz. the sum of p_T of all particles within a cone of 0.2 around the lepton should be less than 10 GeV and the separation from the nearest jet should be less than 0.4. However, these cuts are only fully relevant after parton showering and hadronisation and therefore will be considered in detail in section IV. Therefore, the set of cuts used for the parton-level analysis are:

1. Lepton rapidity : $|\eta| < 2.5$
2. Minimum transverse momenta of the hardest and second hardest leptons : $p_T(\ell_1) > 40$ GeV and $p_T(\ell_2) > 30$ GeV respectively
3. Missing transverse energy: $E_T > 30$ GeV

These cuts suppress the $b\bar{b}$ background completely and reduce the contribution of $Zb\bar{b}$, $Wb\bar{b}$ to very small amounts. The $t\bar{t}$ background is still in the range of several femtobarns and can be further suppressed using a veto on b-tagged jets and also restricting the number of hard jets in the final state. Since both these cuts are dependent on showering and hadronisation effects, we shall examine them only in section IV.

The effect of cuts for SSD on different values of \tilde{b} can be seen in Figure 1. We change only one out of $\text{Re}(\tilde{b})$ and $\text{Im}(\tilde{b})$ at a time. Changing $\text{Re}(\tilde{b})$ increase the p_T of the leptons however, this increase is similar for both $\text{Re}(\tilde{b}) > 0$ and $\text{Re}(\tilde{b}) < 0$. The case for non-zero

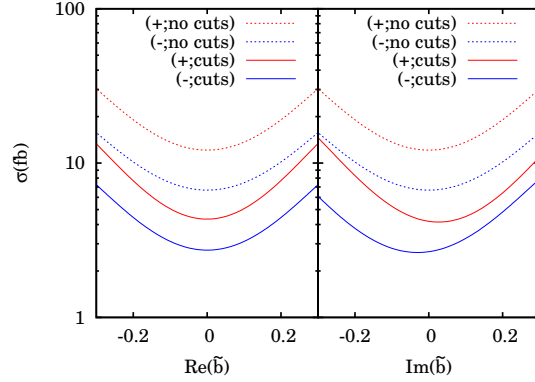


FIG. 1: The behaviour of the cross section ($m_H = 150$ GeV) in the SSD channel for different values of $\text{Re}(\tilde{b})$ and $\text{Im}(\tilde{b})$ (right) and the final cross section after all the cuts. $\text{Im}(\tilde{b})$ is set to zero in the left panel and $\text{Re}(\tilde{b})$ is zero in the right. The dashed line with label “nocuts” refers to the cross section before any cuts are applied whereas the solid lines correspond to the cross section after cuts. The signs \pm refer to the charge of the SSD.

$\text{Im}(\tilde{b})$ however, is different. $\text{Im}(\tilde{b}) < 0$ enhances the p_T for the lepton from W^+ whereas $\text{Im}(\tilde{b}) > 0$ enhances the p_T for the lepton from W^- . This causes an asymmetry in the cross section after the cuts even though there is no asymmetry to start with. This is illustrated in Table I where we present the cut flow table for the SM case and for $\text{Im}(\tilde{b}) = \pm 0.2$ for both $\ell^+\ell^+$ and $\ell^-\ell^-$ final states. The corresponding cross sections with $\text{Re}(\tilde{b}) = 0.2$ for $m_H = 150(130)$ GeV are (7.64)3.49 fb for $\ell^+\ell^+$ and 4.35 (2.08) fb for $\ell^-\ell^-$.

III. NUMERICAL RESULTS

After applying the cuts described in the previous sections, we are left with a fairly pure sample of events. Therefore we shall present the distributions for signal events only. Since the strength of the cross section for different values of the anomalous coupling are already given in Figure 1, we will be presenting only the normalised distributions for the rest of this work. We also present distributions only for Higgs mass (m_H) of 150 GeV since the cross section in this case is larger. The distributions for $m_H = 130$ GeV are qualitatively similar. The asymmetry distributions are shown for both Higgs masses and it will be seen that $m_H = 130$ GeV is in fact more sensitive to some of them.

The first variable of interest is the difference in transverse momenta of the leptons. The

m_H	130 GeV			150 GeV		
$(\tilde{b}; \pm)$	Cut 1	Cut 2	Cut 3	Cut 1	Cut 2	Cut 3
(0.0; +)	3.80	1.56	1.49	5.97	3.06	2.99
(0.0; -)	3.09	1.11	1.06	4.53	2.08	2.02
(0.2i; +)	7.69	2.81	2.77	13.86	6.21	6.16
(0.2i; -)	5.03	2.44	2.30	8.38	4.97	4.77
(-0.2i; +)	7.15	2.81	2.77	12.87	8.66	8.29
(-0.2i; -)	5.28	1.74	1.71	8.75	3.63	3.59

TABLE I: The effect of cuts on the SSD cross section for non-zero $\text{Im}(\tilde{b})$; the \pm signs refer to the charge of the SSD. The cross sections are in fb and are evaluated at $\sqrt{s} = 14$ TeV. The cuts are explained in the text.

two leptons in the SSD channel are labeled in descending order of their p_T . We then define $\Delta p_T = p_T^{(1)} - p_T^{(2)}$. The charge of the SSD points out whether we have a W^+ or W^- initiated process. Figure 2 shows the distribution for both W^\pm -type processes. The sign of $\text{Re}(\tilde{b})$ does not affect the hardness of the distribution. Therefore, we show only one curve corresponding to $\text{Re}(\tilde{b}) = 0.2$. However, the difference due to change in sign of $\text{Im}(\tilde{b})$ is reflected in the two curves corresponding to $\text{Im}(\tilde{b}) = \pm 0.2$.

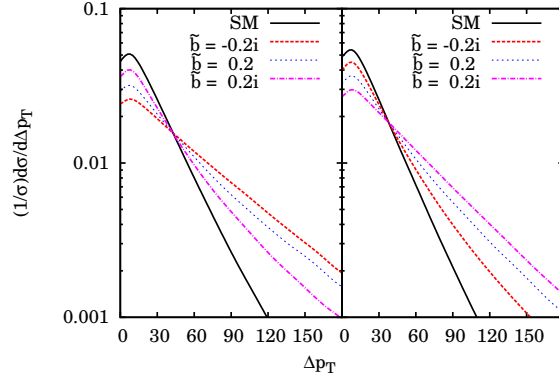


FIG. 2: The normalised Δp_T distribution between two same-sign leptons for $m_H = 150$ GeV. The left(right) panel corresponds to $\ell^+\ell^+$ ($\ell^-\ell^-$)-type process.

Next, we consider the distribution in the angle between the two same-sign leptons. In the absence of any cuts, the distribution peaks at $\theta = 0$, i.e. $\cos\theta = 1$. However, the p_T

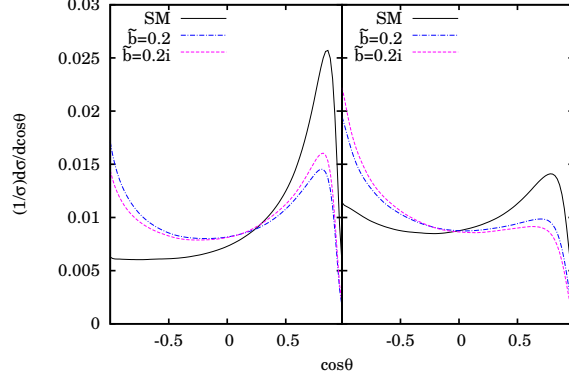


FIG. 3: The normalised distribution of cosine of the angle between two same-sign leptons for $m_H = 150$ GeV. The effect of changing either $\text{Re}(\tilde{b})$ or $\text{Im}(\tilde{b})$ is to enhance the back-to-back nature of the leptons. The left panel shows the $\ell^+\ell^+$ whereas the right panel shows the $\ell^-\ell^-$ -type distributions.

cuts remove nearly all these highly collinear events. The peak for SM curve is shifted from $\cos\theta = 1$ to $\cos\theta \sim 0.5$. Figure 3 shows how the distribution changes for non zero $\text{Re}(\tilde{b})$ and $\text{Im}(\tilde{b})$. The effect of the anomalous coupling is to enhance the back-to-back nature of the distribution. The forward peak is almost completely diminished. A quantitative measure of this change can be made by measuring the asymmetry around $\cos\theta = 0$.

We then look at the $\Delta\phi$ distribution, where $\Delta\phi$ is defined as $\phi_{\ell_1} - \phi_{\ell_2}$ and ϕ stands for the azimuthal angle. In this case however, we adopt a different ordering of the leptons. We wish to identify which lepton is more likely to come from Higgs decay (ℓ_2) and which from the main hard interaction (ℓ_1). Since one of the W s from the Higgs decays into jets, we would expect the lepton from Higgs decay to be closer to at least one of the jets than the other lepton. We therefore pick the lepton with the smallest distance to any of the jets as ℓ_2 and then construct $\Delta\phi$. Contrary to the previous distributions, this distribution is particularly sensitive to the sign of $\text{Re}(\tilde{b})$ but not to the sign of $\text{Im}(\tilde{b})$. The effect of different $\text{Re}(\tilde{b})$ on both $\ell^+\ell^+$ and $\ell^-\ell^-$ can be seen from Figure 4. A non-zero $\text{Im}(\tilde{b})$ only changes the height of the dip and the distribution is symmetric about $\Delta\phi = 0$ whereas flipping the sign of $\text{Re}(\tilde{b})$ flips the distribution as well.

Since the $\Delta\phi$ distribution has a central dip and also shows left-right symmetry for the

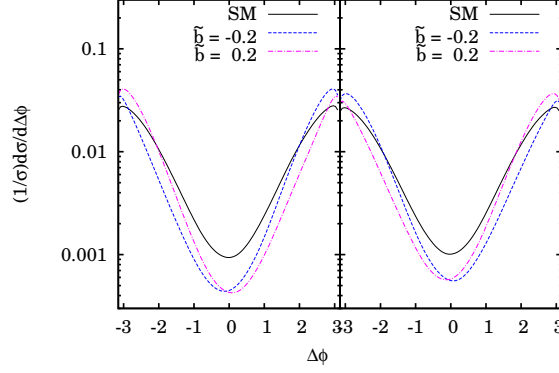


FIG. 4: Effect of positive (dashed) and negative (dot-dashed) values of $\text{Re}(\tilde{b})$ on the $\Delta\phi$ distributions for $m_H = 150$ GeV. The left panel corresponds to $\ell^+\ell^+$ and the right to $\ell^-\ell^-$ final states.

standard model case, we can construct two kinds of asymmetries, viz.

$$A_{SSD1} = \frac{\sigma(\Delta\phi > 0) - \sigma(\Delta\phi < 0)}{\sigma(\Delta\phi > 0) + \sigma(\Delta\phi < 0)} \quad (2)$$

$$A_{SSD2} = \frac{\sigma(|\Delta\phi| < \pi/2) - \sigma(|\Delta\phi| > \pi/2)}{\sigma(|\Delta\phi| < \pi/2) + \sigma(|\Delta\phi| > \pi/2)} \quad (3)$$

The first is a left-right asymmetry which captures the change in the sign of $\text{Re}(\tilde{b})$ but remains unaffected by $\text{Im}(\tilde{b})$. The effect of $\text{Re}(\tilde{b})$ on A_{SSD1} is shown in Figure 5. The sign of the asymmetry is oppositely correlated to the sign of the coupling. We also look at A_{SSD2} distribution given in Figure 6 which describes how central the $\Delta\phi$ distribution is. We notice that the effect of both $\text{Re}(\tilde{b})$ and $\text{Im}(\tilde{b})$ is similar in this regard. Therefore if A_{SSD2} shows a significant deviation from the SM value but A_{SSD1} does not, it would point to the presence of a non zero $\text{Im}(\tilde{b})$.

For a reasonable estimation at the LHC, we require that the asymmetries be reasonable separated from the SM value by at least three standard deviations. Using the formula in equation (5), for a value of $\text{Re}(\tilde{b}) = 0.2$ and $m_H = 150$ GeV for $\ell^+\ell^+$ -type events, we find that a luminosity of 30fb^{-1} gives an asymmetry $A_{SSD1} = -0.210 \pm 0.065$ and $A_{SSD2} = -0.886 \pm 0.031$, both of which are inconsistent with the SM values of $A_{SSD1} = -0.002$ and $A_{SSD2} = -0.786$ by the required factor. A 5σ difference can be achieved with 50fb^{-1} data. The corresponding 3σ measurement for $m_H = 130$ GeV can be done with 50fb^{-1} giving $A_{SSD1} = -0.222 \pm 0.074$ and $A_{SSD2} = -0.88 \pm 0.036$. A 5σ measurement would require 140fb^{-1} .

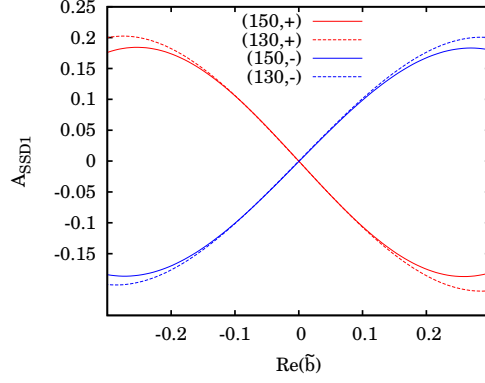


FIG. 5: The asymmetry A_{SSD1} for different values of $\text{Re}(\tilde{b})$ for $\ell^+\ell^+$ (red) and $\ell^-\ell^-$ (blue) with $\text{Im}(\tilde{b}) = 0$. The labels refer to the Higgs mass and the sign of the SSD.

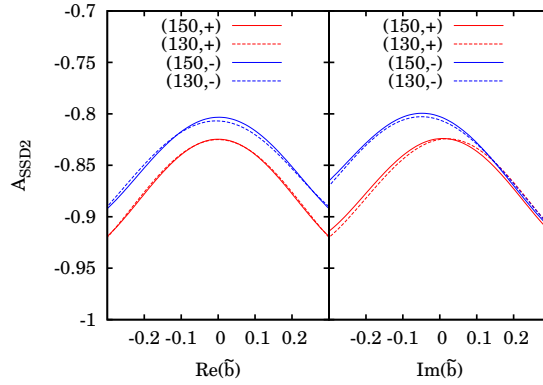


FIG. 6: The asymmetry A_{SSD2} for different values of the anomalous couplings. The labels indicate the Higgs mass and the sign of the SSD.

To complement the $\Delta\phi$ variable which is sensitive to the sign of $\text{Re}(\tilde{b})$, we would also like to construct a variable that is sensitive to the sign of $\text{Im}(\tilde{b})$. We first reconstruct the W that has decayed into jets and obtain its rapidity, η_W . We then construct $\Delta\eta = |\eta_1 - \eta_W| - |\eta_2 - \eta_W|$. Where $\eta_{1,2}$ are the rapidities of the leptons ordered in the descending order of p_T . We use the difference from η_W to make the variable invariant under Lorentz boosts in the beam direction. This variable is most likely to be modified after taking into account initial and final state radiation (ISR and FSR) effects as the number of jets are modified. We shall deal with this concern in Section IV.

We also construct a similar variable, $\Delta|\eta| = |\eta_1| - |\eta_2|$ which shows sensitivity to $\text{Im}(\tilde{b})$

and is much less sensitive to $\text{Re}(\tilde{b})$. It also has the added advantage that one need not reconstruct the W and therefore can look into inclusive SSD final states and is therefore expected to be more robust to FSR effects. However, it should be noted that this variable is not invariant under longitudinal boosts.

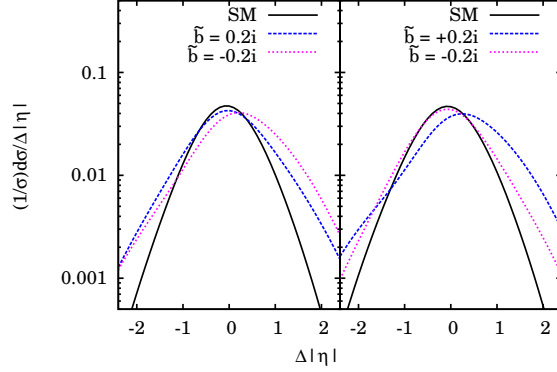


FIG. 7: Effect of positive (dashed) and negative (dot-dashed) values of $\text{Im}(\tilde{b})$ on the $\Delta\eta$ distributions for $m_H = 150$ GeV. The left panel corresponds to $\ell^+\ell^+$ and the right to $\ell^-\ell^-$ final states.

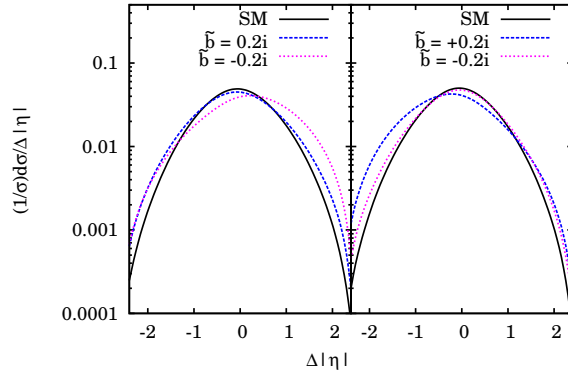


FIG. 8: Effect of positive (dashed) and negative (dot-dashed) values of $\text{Im}(\tilde{b})$ on the $\Delta|\eta|$ distributions for $m_H = 150$ GeV. The left panel corresponds to $\ell^+\ell^+$ and the right to $\ell^-\ell^-$ final states.

The distributions of $\Delta\eta$ and $\Delta|\eta|$ are shown in Figure 7 and 8 respectively. In both the cases, the $\ell^+\ell^+$ final state is particularly sensitive to $\text{Im}(\tilde{b}) < 0$ whereas the $\ell^-\ell^-$ one is sensitive to $\text{Im}(\tilde{b}) > 0$. Therefore, we can use these variables to confirm the presence of a non-zero $\text{Im}(\tilde{b})$ as only one of $\ell^+\ell^+$ or $\ell^-\ell^-$ will show a significant deviation from the SM

value. The first variable is useful because it shows a larger asymmetry and can therefore be used with lower luminosity. However, the shift in the curve is independent of the sign of $\text{Im}(\tilde{b})$. The second variable on the other hand, has a lower asymmetry but changes sign depending on the sign of $\text{Im}(\tilde{b})$. We also find that the effect of non-zero $\text{Re}(\tilde{b})$ is much smaller and is un-correlated with the its sign. Here too, we can construct left-right asymmetries to better parametrise this difference.

$$A_{SSD3} = \frac{\sigma(\Delta\eta > 0) - \sigma(\Delta\eta < 0)}{\sigma(\Delta\eta > 0) + \sigma(\Delta\eta < 0)} \quad (4)$$

$$A_{SSD4} = \frac{\sigma(\Delta|\eta| > 0) - \sigma(\Delta|\eta| < 0)}{\sigma(\Delta|\eta| > 0) + \sigma(\Delta|\eta| < 0)} \quad (5)$$

The distribution of the asymmetry A_{SSD3} for different values of $\text{Re}(\tilde{b})$ and $\text{Im}(\tilde{b})$ is shown in Figure 9. We can see that $\text{Re}(\tilde{b})$ affects both $\ell^+\ell^+$ or $\ell^-\ell^-$ symmetrically whereas $\text{Im}(\tilde{b})$ shows a very pronounced asymmetry depending on sign. For $\ell^+\ell^+$ events observed with an integrated luminosity of $30(50) \text{ fb}^{-1}$ and $\tilde{b} = -0.2i$, we get an asymmetry $A_{SSD3} = 0.288 \pm 0.061(0.241 \pm 0.070)$ for $m_H = 150(130) \text{ GeV}$ with as compared to the SM value of -0.01 (same for both Higgs masses). The distribution of A_{SSD4} is shown in Figure 10. The left panel shows the dependence on $\text{Re}(\tilde{b})$. The asymmetry distribution is symmetric with respect to its sign but is of opposite sign for $\ell^+\ell^+$ and $\ell^-\ell^-$ states. The right panel shows the effect of $\text{Im}(\tilde{b})$. We see that in this case as well, the sign of $\text{Im}(\tilde{b})$ causes pronounced asymmetry in either $\ell^+\ell^+$ or $\ell^-\ell^-$ states. This asymmetry can therefore supplement the conclusions from A_{SSD3} . For $\ell^+\ell^+$ states with $\tilde{b} = -0.2i$ and $30(50) \text{ fb}^{-1}$ integrated luminosity, A_{SSD4} takes the values $0.217 \pm 0.062(0.191 \pm 0.071)$ for $m_H = 150(130) \text{ GeV}$.

In all we find that the presence of anomalous couplings makes the Δp_T distribution harder and enhances the back-to-back region in the $\cos\theta$ distribution. Since the reliable construction of the asymmetries requires accumulation of a large data set, we first test the presence of anomalous couplings using these two distributions. We can then use the three asymmetry variables to for positive and negative SSD to determine what kind of anomalous coupling is present. Let the labels (+) and (−) refer to the charge of the SSD. Then we can conclude the following:

- $A_{SSD1}(\pm) = 0 \Rightarrow \text{Re}(\tilde{b}) = 0$
- $A_{SSD1}(+) \neq 0 \Rightarrow \text{Re}(\tilde{b}) \neq 0; \text{sign}(\text{Re}(\tilde{b})) = -\text{sign}(A_{SSD1}(+))$

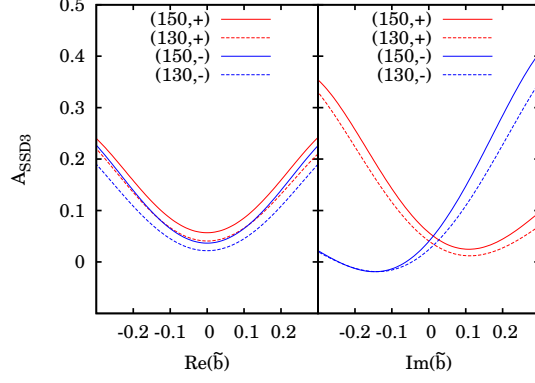


FIG. 9: The asymmetry A_{SSD3} for different values of the anomalous couplings. The labels indicate the Higgs mass and the sign of the SSD.

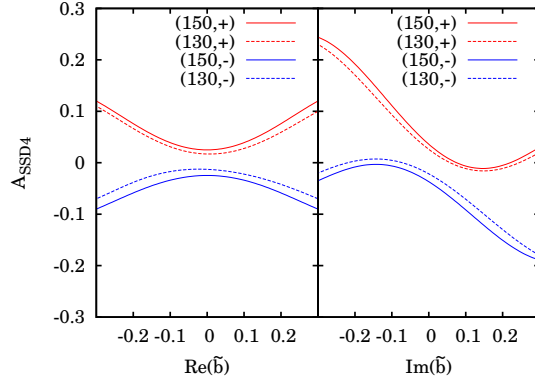


FIG. 10: The asymmetry A_{SSD4} for different values of the anomalous couplings. The labels indicate the Higgs mass and the sign of the SSD.

- $|A_{SSD3,SSD4}(+)| < |A_{SSD3,SSD4}(-)| \Rightarrow \text{Im}(\tilde{b}) > 0$
- $|A_{SSD3,SSD4}(+)| > |A_{SSD3,SSD4}(-)| \Rightarrow \text{Im}(\tilde{b}) < 0$

Since the asymmetry variables listed above are not explicitly CP-violating, it is possible that they might also be affected by the presence of CP-conserving anomalous coupling b . We therefore wish to determine if it is possible to get similar results from a non-zero value of b and whether it is possible to distinguish the effect of the two kinds of couplings.

We perform a similar calculation of $pp \rightarrow h\ell\nu$ and $h \rightarrow \ell\nu jj$ using the HWW vertex given in equation 1 with $\tilde{b} = 0$ instead. The cross section of Higgs production after including b is then required to also be within the Tevatron bounds. This corresponds to a value of

$|b| \leq 0.05$ which will be used for the rest of this section. We then examine the three asymmetries defined in the previous section with the same cuts.

We find that the $\Delta\phi$ asymmetry A_{SSD1} and the $\Delta|\eta|$ -based A_{SSD4} are both completely unaffected by the presence of b . Therefore, these two together can constitute robust variables at the LHC for confirming the presence of a CP-violating anomalous HWW coupling. The second $\Delta\phi$ -based asymmetry, A_{SSD2} is more negative in the case of CP-conserving anomalous couplings. However, the difference is small and measuring it with accuracy will require a large luminosity. The $\Delta\eta$ -based A_{SSD3} shows similar behaviour between non zero values b and $\text{Im}(\tilde{b})$. We can further discriminate between b or \tilde{b} type coupling by examining the Δp_T distribution which falls off much slower in the case of the CP conserving coupling. This can set apart the presence of $\text{Im}(\tilde{b})$ quite distinctly. As an illustration, we present a comparison in Figure 11. We find that difference in the distributions for $b > 0$ ($b < 0$) is probed best in $\ell^+\ell^+$ ($\ell^-\ell^-$) channels irrespective of the sign of $\text{Im}(\tilde{b})$. In both cases, we find the distributions are distinct enough to allow us to separate the effects from the two couplings.

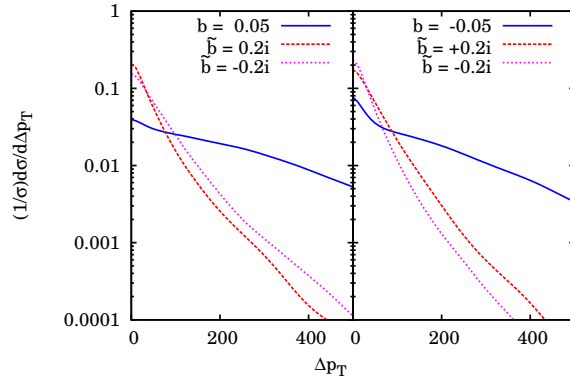


FIG. 11: Comparison of the normalised Δp_T distribution between two same-sign leptons for $m_H = 150$ GeV for values of b and \tilde{b} . The left(right) panel corresponds to $\ell^+\ell^+$ ($\ell^-\ell^-$)-type process.

IV. EFFECT OF SHOWERING AND HADRONISATION

Until now we have been working under the simplified scheme of parton-level Monte-Carlo analysis. However, initial and final-state radiation play a very important role at the LHC. In particular the entire partonic system can acquire a transverse momentum due to recoil

from ISR. One therefore needs to examine whether the effects of showering destroy the correlations we had examined in the previous section. In this section, we investigate this in the context of the distributions and asymmetries defined above.

We have started by obtaining unweighted events from the parton-level code, which are then passed through PYTHIA8[29, 30] using the LHEF file format[31]. PYTHIA8 performs the initial and final state showers and hadronisation after which we use FastJet 2.4.1 with the anti-kt algorithm[32] with a cone size parameter of 0.4 to form the jets. Leptons are considered isolated if the sum of E_T of particles around the lepton within a cone of 0.2 is less than 10 GeV and the separation with the nearest jet is greater than 0.4. All the variables and asymmetries are defined as before.

As an illustration, we first present the $\Delta\phi$ distributions for a $\ell^+\ell^-$ final state for a value of $\tilde{b} = 0.2$ in Figure 12. It can be seen that the distribution retains the correct left-right asymmetry. The $\Delta\eta$ distribution for $\ell^-\ell^-$ and a value of $\tilde{b} = 0.2i$ is shown in Figure 13 and the $\Delta|\eta|$ distribution is shown in Figure 14. In these cases too, we see that the distribution is fairly unchanged. Both these distributions can therefore be thought of as robust variables for LHC analyses.

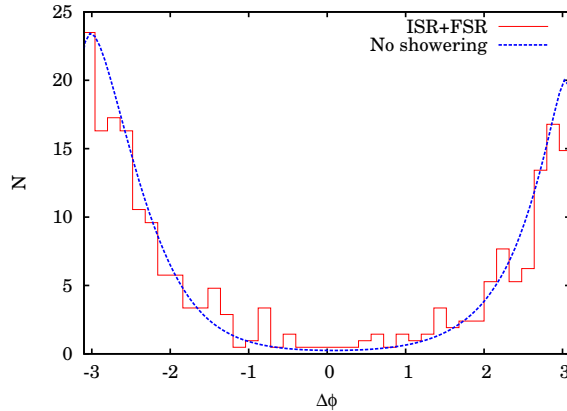


FIG. 12: Comparison of the $\Delta\phi$ distribution before and after including ISR and FSR for $\ell^+\ell^-$ final states and a value of $\tilde{b} = 0.2$ and $m_H = 150$ GeV for 30 fb^{-1} .

We also present the values of the asymmetry variable constructed in the previous sections in Table II. The variable A_{SSD1} is the most robust as the values change only very slightly. The $\Delta\eta$ dependent A_{SSD3} still shows an asymmetry based on sign of $\text{Im}(\tilde{b})$ but the effect is diluted after taking ISR effects into account.

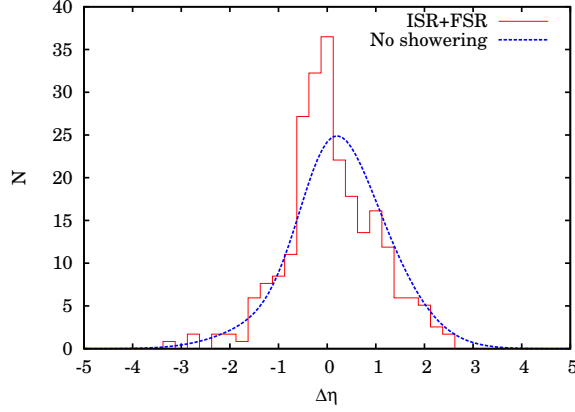


FIG. 13: Comparison of the $\Delta\eta$ distribution before and after including ISR and FSR for $\ell^-\ell^-$ final states and a value of $\tilde{b} = 0.2i$ and $m_H = 150$ GeV for 30 fb^{-1} .

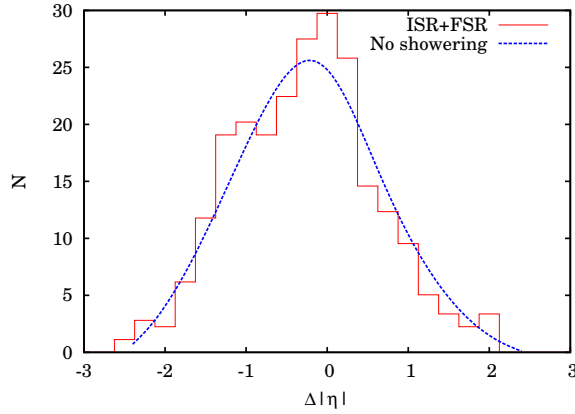


FIG. 14: Comparison of the $\Delta|\eta|$ distribution before and after including ISR and FSR for $\ell^-\ell^-$ final states and a value of $\tilde{b} = 0.2i$ and $m_H = 150$ GeV for 30 fb^{-1} .

V. CONCLUSIONS

We have systematically examined the effects of a CP-violating HWW coupling on Higgs production and decay at the LHC. We probe this coupling via the WH associated production followed by $H \rightarrow WW^* \rightarrow \ell\nu f\bar{f}'$ which gives rise to same-sign dilepton final states. We take into account the Tevatron limits on the Higgs cross section to restrict the values of real and imaginary parts of the anomalous coupling. We find that, besides enhancing the production cross section, it also causes significant deviations in various kinematic correlations between leptons in the final state.

We have presented several variables whose distributions show significant deviation from

	$\tilde{b} = 0$	$\tilde{b} = 0.2$	$\tilde{b} = -0.2$	$\tilde{b} = 0.2i$	$\tilde{b} = -0.2i$
$A_{SSD1} W^+$	0.03(0.00)	-0.27(-0.21)	0.19(0.21)	0.08(0.00)	-0.07(0.00)
W^-	-0.08(0.00)	0.27(0.20)	-0.19(-0.20)	-0.03(0.00)	0.03(0.00)
$A_{SSD2} W^+$	-0.73(-0.79)	-0.82(-0.89)	-0.80(-0.87)	-0.76(-0.88)	-0.77(0.87)
W^-	-0.61(-0.77)	-0.78(-0.86)	-0.80(-0.86)	-0.78(-0.88)	-0.70(-0.83)
$A_{SSD3} W^+$	0.05(-0.01)	0.06(0.17)	0.06(0.17)	0.03(0.04)	0.12(0.31)
W^-	0.02(-0.03)	0.10(0.15)	0.06(0.15)	0.12(0.29)	0.03(0.02)
$A_{SSD4} W^+$	-0.01(-0.01)	0.02(0.08)	0.04(0.08)	-0.01(-0.01)	0.13(0.22)
W^-	-0.05(-0.01)	-0.08(-0.06)	-0.14(-0.06)	-0.11(-0.17)	-0.03(-0.01)

TABLE II: Asymmetries after ISR and FSR for $m_H = 150$ GeV. The value from parton-level calculations is given in the parentheses for comparison.

the standard model case. We also define asymmetries constructed from three of them, viz. $\Delta\phi$, $\Delta\eta$ and $\Delta|\eta|$, which can show significant deviation from SM predictions. Trends in the Δp_T and $\cos\theta$ distributions may be used to first ascertain the presence of an anomalous coupling. The left-right asymmetry in the $\Delta\phi$, $\Delta\eta$ and $\Delta|\eta|$ distributions can be used to probe its nature in detail. After imposing cuts required to suppress the SM backgrounds, the asymmetries can be discerned at the $3(5)\sigma$ level at 14 TeV, with an integrated luminosity of $30(50) \text{ fb}^{-1}$ for a Higgs of mass 150 TeV. The asymmetries for a Higgs mass of 130 GeV can be similarly determined at $3(5)$ sigma with $50(140) \text{ fb}^{-1}$. It should be noted that our calculation is done at the leading order, and the inclusion of an appropriate next-to-leading order K-factor is expected to enhance the signal rates. We also present and compare various distributions at the parton level and after showering and hadronisation. We find that our conclusions are largely unchanged, even after taking the latter effects into account.

Acknowledgments

ND and BM are partially supported by funding available from the Department of Atomic Energy, Government of India for the Regional Centre for Accelerator-based Particle Physics(RECAP), Harish-Chandra Research Institute. DKG acknowledges partial support from the Department of Science and Technology, India under the grant SR/S2/HEP-12/2006.

ND and BM also thank the Indian Association for the Cultivation of Science for hospitality at the initial stage of this work. DKG acknowledges the hospitality the Abdus Salam International Centre for Theoretical Physics and RECAPP at a later stage of the project. Computational work for this study was partially carried out at the cluster computing facility of Harish-Chandra Research Institute (<http://cluster.mri.ernet.in>).

-
- [1] CDF and DØ Collaborations (2010), 1007.4587.
 - [2] J. Baglio, A. Djouadi, S. Ferrag, and R. Godbole (2011), 1101.1832.
 - [3] G. Bayatian et al. (CMS Collaboration), J.Phys.G **G34**, 995 (2007).
 - [4] G. Aad et al. (The ATLAS Collaboration) (2009).
 - [5] B. Zhang, Y.-P. Kuang, H.-J. He, and C. Yuan, Phys.Rev. **D67**, 114024 (2003).
 - [6] S. S. Biswal, R. M. Godbole, R. K. Singh, and D. Choudhury, Phys. Rev. **D73**, 035001 (2006).
 - [7] R. M. Godbole, . Miller, D.J., and M. Muhlleitner, JHEP **0712**, 031 (2007).
 - [8] Y.-H. Qi, Y.-P. Kuang, B.-J. Liu, and B. Zhang, Phys.Rev. **D79**, 055010 (2009).
 - [9] Z. Zhang, G.-M. Chen, M. Yang, B.-J. Liu, J.-Q. Tao, et al., Phys.Rev. **D78**, 073010 (2008).
 - [10] T. Han and Y. Li, Phys.Lett. **B683**, 278 (2010).
 - [11] N. D. Christensen, T. Han, and Y. Li, Phys.Lett. **B693**, 28 (2010).
 - [12] . Miller, D.J., S. Choi, B. Eberle, M. Muhlleitner, and P. Zerwas, Phys.Lett. **B505**, 149 (2001), hep-ph/0102023.
 - [13] S. Choi, . Miller, D.J., M. Muhlleitner, and P. Zerwas, Phys.Lett. **B553**, 61 (2003), hep-ph/0210077.
 - [14] S. D. Rindani and P. Sharma, Phys.Rev. **D79**, 075007 (2009).
 - [15] S. S. Biswal, D. Choudhury, R. M. Godbole, and Mamta, Phys.Rev. **D79**, 035012 (2009), 0809.0202.
 - [16] S. S. Biswal and R. M. Godbole, Phys.Lett. **B680**, 81 (2009).
 - [17] Y. Takubo et al. (2010), 1011.5805.
 - [18] D. Choudhury and Mamta, Phys.Rev. **D74**, 115019 (2006).
 - [19] T. Han, Y.-P. Kuang, and B. Zhang, Phys.Rev. **D73**, 055010 (2006).
 - [20] B. Sahin, J.Phys.G **G36**, 025012 (2009).
 - [21] M. Acciarri et al. (L3 Collaboration), Phys.Lett. **B489**, 102 (2000).

- [22] M. Dittmar and H. K. Dreiner, Phys.Rev. **D55**, 167 (1997).
- [23] V. Hankele, G. Klamke, D. Zeppenfeld, and T. Figy, Phys.Rev. **D74**, 095001 (2006).
- [24] T. Arens, U. Gieseler, and L. Sehgal, Phys.Lett. **B339**, 127 (1994).
- [25] J. Vermaseren (2000), math-ph/0010025.
- [26] J. Pumplin et al., JHEP **07**, 012 (2002).
- [27] CDF Collaboration (2011),
http://www-cdf.fnal.gov/physics/new/hdg//Results_files/results/hwwmenn_110304/.
- [28] Z. Sullivan and E. L. Berger, Phys.Rev. **D82**, 014001 (2010).
- [29] T. Sjostrand, S. Mrenna, and P. Z. Skands, Comput.Phys.Commun. **178**, 852 (2008).
- [30] T. Sjostrand, S. Mrenna, and P. Z. Skands, JHEP **0605**, 026 (2006).
- [31] J. Alwall et al., Comput.Phys.Commun. **176**, 300 (2007).
- [32] M. Cacciari, G. P. Salam, and G. Soyez, JHEP **04**, 063 (2008).
- [33] B. Mellado; private communication